ELSEVIER

Thin Solid Films 424 (2003) 45–49

thin solid films

www.elsevier.com/locate/tsf

Motion and conversion energies of adatom and adatom clusters on gold (0 0 1) surface☆

J. Takano[1], Masao Doyama*, Y. Kogure

Teikyo University of Science and Technology, Uenohara, Yamanashi 409-0193, Japan

Abstract

Beginning of epitaxial growth of vapor deposition on (0 0 1) surface has been studied by use of molecular dynamics. The activation energies of motion and conversion can be calculated using an embedded atom potential at any temperatures. The activation energy of the motion of a gold adatom on (0 0 1) surface of gold is calculated to be 0.41 eV. The activation energies of dissociation in the direction of a di-adatom is 0.72 eV from the nearest neighbor to the next nearest neighbor, and 0.27 eV from the next nearest neighbor to the third neighbor. Butterfly motion of a di-adatom is 0.42 + 0.12 eV = 0.54 eV. Tri-adatoms are classified by the angle between the two bonds in the adatoms and the lengths of the two bonds. The conversion energies of tri-adatoms have also been calculated. The activation energy for the motion of an adatom on (0 0 1) surface is much higher than those corresponding the motion on (1 1 1) surfaces.

Keywords: Conversion energies; Activation energy; Adatom clusters

1. Introduction

Surface phenomena are becoming more important in view of technical applications as well as basic science. The crystal growth of surfaces by epitaxial growth is widely used by electronic industries. Surface diffusion is very important for this process. In the present study to understand the microscopic mechanism of thin film growth process, various motions of atoms on the substrates are simulated. It was found [1] that the migration energy of a gold adatom on (1 1 1) surface is very low, nearly 0.055 eV from a normal site to a hexagonal site and 0.042 eV from a hexagonal site to a normal site. The activation energy for the motion of a di-adatom was found to be 0.12 eV. The migration energies and conversion energies of a copper adatom clusters on (1 1 1) are higher than 0.1 eV. The migration of a single adatom on (1 1 1) is much easier than the migration of adatom clusters [1,2].

2. Classification and nomenclature of adatom clusters

We denote an adatom, a di-adatom, a tri-adatom, etc. as I, II, III, etc. The lengths of the bonds in adatom clusters are represented by subscripts and the angle between the bonds by superscript. d is the nearest neighbor distance. Tri-adatoms can be represented by 'dog legs' [3]. These can be represented by the angle between two bonds as a superscript and the lengths of the bonds as subscripts.

3. Interatomic potential

In metals, the conduction electrons travel from one atom to another atom and the interaction between atoms cannot be represented by a pairwise potential but by many body potentials. The interaction between the ith atom and the jth atom depends not only on the distance between them but also on other factors. By the embedded function [4–9], surface problems can be also treated.

☆ This paper is based on a part of the Ph.D. (in Advanced Science and Technology) thesis, Teikyo University of Science and Technology by J. Takano (2002).

*Corresponding author. Tel.: +81-554-63-44-11; fax: +81-554-63-44-31.

E-mail address: doyama@ntu.ac.jp (M. Doyama).

[1] Present address: Science and Technology Foresight Center (STFC), National Institute of Science and Technology Policy (NISTEP), Ministry of Education, Culture, Sports, Science and Technology (MEXT), 1-3-2, Kasumigaseki, Chiyoda-ku, Tokyo 100-0013, Japan.

0040-6090/03/$ - see front matter © 2002 Elsevier Science B.V. All rights reserved.
PII: S0040-6090(02)00905-7

The N-body embedded function used in this paper can be found in Ref. [9].

4. Activation energies for motion and conversion

A rectangular parallelepiped crystal bounded by six {1 0 0} planes was prepared. The *x*-, *y*- and *z*-axes are taken to be the [1 0 0], [0 1 0] and [0 0 1] directions, respectively. The length in the *x* direction is 10*a*, in the *y* direction 8*a* and in the *z* direction 4*a*, where *a* is the lattice parameter, and the crystal contains 1584 atoms. Adatoms were added near the (0, 0, 0) *x*, *y* and *z* position, the center of (0 0 1) surface. Two hundred and eighty atoms near adatom clusters in the original crystal and adatom clusters were relaxed. This region is called Region I. The activation energies for the motion, conversion and break-up of adatom clusters have been calculated (Fig. 1). All atoms in Region I are relaxed except the *x*- and *y*-coordinates of the moving atom on a predicted moving line are fixed but the *z*-coordinate is relaxed. Molecular dynamics are used for relaxation. The crystal energies of Region I along a path of conversion or motion are also plotted in Fig. 1. Motion and conversion energies of an adatom and adatom clusters are also shown in Fig. 1.

4.1. Adatom

The activation energy for the motion of an adatom on (0 0 1) was calculated to be 0.41 eV [I→I] (Fig. 1a).

4.2. Di-adatoms

Activation energies of separation of a di-adatom in a perpendicular direction [$II_d \rightarrow II_{\sqrt{2}d}$] was calculated to be 0.42 eV (Fig. 1b). Activation energies of trapping motion of a di-adatom [$II_{\sqrt{2}d} \rightarrow II_d$] was calculated to be 0.12 eV (Fig. 1b). A butterfly motion [$II_d \rightarrow II_d$] from (−1, 1, 0)–(0, 0, 0) to (0, 0, 0)–(1, 1, 0), requires 0.54 eV (=0.42+0.12). Activation energy of break-up of a di-adatom [$II_d \rightarrow II_{2d}$] was calculated to be 0.72 eV [$II_d \rightarrow II_{2d}$] (Fig. 1c). Activation energy of trapping motion of a di-adatom [$II_{2d} \rightarrow II_d$] was calculated to be 0.27 eV.

4.3. Tri-adatoms

Activation energies of separation of a tri-adatom in a perpendicular direction [$III^{180}_{2\times d} \rightarrow III^{135}_{d,\sqrt{2}d}$] were calculated to be 0.43 eV, which is almost the same as the corresponding case of a di-adatom (0.42 eV) [$II_d \rightarrow II_{\sqrt{2}d}$] and 0.50 eV for the motion [$III^{135}_{d,\sqrt{2}d} \rightarrow III_{d,\sqrt{5}d}$]. Activation energy of separation of a tri-adatom [$III^{180}_{2\times d} \rightarrow III^{180}_{d,2d}$] was calculated to be 0.69 eV (Fig. 1e), which is almost equal to the corresponding case of di-adatom (0.72 eV). Activation energy of trapping motion of a tri-adatom [$III^{180}_{d,2d} \rightarrow III^{180}_{2\times d}$] was calculated to be 0.27 eV compared with corresponding 0.27 eV for a di-adatom [$II_{2d} \rightarrow II_d$]. Activation energy of separation of a tri-adatom [$III^{180}_{d,2d} \rightarrow III^{180}_{d,3d}$] was calculated to be 0.37 eV (Fig. 1e). Activation energies of trapping motion of a tri-adatom [$III_{d,\sqrt{5}d} \rightarrow III_{d,\sqrt{2}d}$] were calculated to be 0.35 and 0.16 eV for the trapping motion [$III_{d,\sqrt{2}d} \rightarrow III_{2\times d}$]. The activation energies of motion III^{180}(0, 0, 0)–(−1, 1, 0)–(−2, 2, 0)→III(1, 1, 0)–(−1, 1, 0)–(−2, 2, 0) is 0.43 eV which is almost the same as the case of a di-adatom (0.42 eV) and the motion of a single adatom. The activation energy of conversion [$III^{180}_{2\times d} \rightarrow III^{90}_{2\times\sqrt{2}d}$] the motion from (−1, 1, 0)–(0, 0, 0)–(1, −1, 0) to (1, −1, 0)–(1, 1, 0)–(1, −1, 0) (Fig. 1f) is 0.54 eV and the reaction [$III^{90}_{2\times\sqrt{2}d} \rightarrow III^{52}_{2\times\sqrt{5}d}$] is 0.68 eV. The trapping energy [$III^{90}_{2\times\sqrt{2}d} \rightarrow III^{180}_{2\times d}$] is 0.02 eV, which is very low. The energy of separation $III^{90}_{2\times d} \rightarrow III^{90}_{d,2d}$ is 0.83 eV (Fig. 1g). The trapping energies [$III^{90}_{d,2d} \rightarrow III^{90}_{2\times d}$] is 0.28 eV (Fig. 1g). The activation energies of conversion [$III^{90}_{d,2d} \rightarrow III^{90}_{d,3d}$] and [$III^{90}_{d,3d} \rightarrow III^{90}_{d,2d}$] are both 0.37 eV (Fig. 1g). The activation energy of conversion from [$III^{90}_{2\times d} \rightarrow III^{90}_{2\times d}$] is 0.19 eV (Fig. 1h), which is also low and [$III^{90}_{2\times d} \rightarrow III^{135}_{d,\sqrt{2}d}$] is 0.56 eV. The trapping [$III^{135}_{d,\sqrt{2}d} \rightarrow III^{90}_{2\times d}$] (Fig. 1h) is 0.35 eV.

5. Vibrational frequencies and jump frequencies of a single adatom and adatom clusters

From the curvature of the crystal energy of Region I against the positions near a stable or a meta-stable position, the thermal frequency of an adatom at a stable point for an adatom was calculated to be 1.23×10^{12} s^{-1}. The frequency of the (0, 0, 0) atom of a di-adatom (−1, 1, 0)–(0, 0, 0) in the [1 1 0] direction was 1.03×10^{12} s^{-1} and that of (1, 1, 0) atom of the (−1, 1, 0) and (1, 1, 0) is 1.1×10^{12} s^{-1}. The positions of atoms are represented by the *x*-, *y*- and *z*-coordinates. The vibrational frequencies of the atom of (0, 0, 0) atom of a tri-adatom (−2, 2, 0)–(−1, 1, 0)–(0, 0, 0) is 1.74×10^{12} s^{-1}. Other frequencies can be found in Table 1. In Table 1, some of the frequencies of the atom in an adatom clusters are shown and the jump frequencies at 0, 300 and 500 °C are also listed.

6. Discussions

6.1. Activation energies for the surface diffusion and conversion energies

In this paper, activation energies of motions and conversions of adatoms and adatom clusters have been calculated using embedded atom potential. Surface reconstructions were not taken into account. To treat this problem, ab initio calculation should be used in the future. The value of the activation energy for the

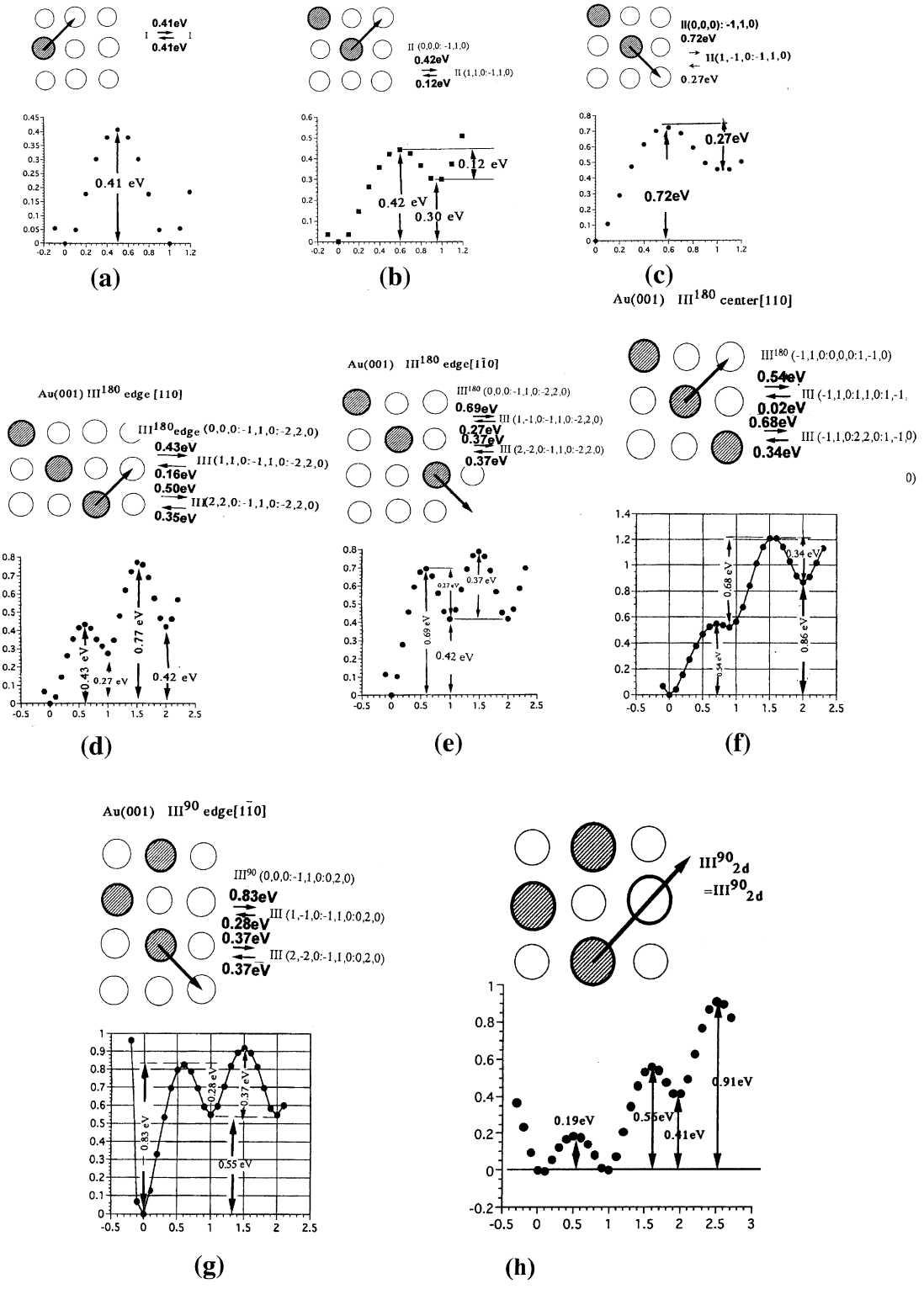

Fig. 1. Examples of adatom clusters on (0 0 1). Abscissa is the distance in the nearest neighbor distance unit and the ordinate represents the crystal energy in electron volts. (a) $I \rightarrow I$; (b) $II_d \rightarrow II_{\sqrt{2}d}$; (c) $II_d \rightarrow II_{2d}$; (d) $III^{180}_{2\times d} \rightarrow III^{135}_{d,\sqrt{2}d}$; (e) $III^{180}_{2\times d} \rightarrow III^{180}_{d,2d,}$; (f) $III^{180}_{2\times d} \rightarrow III^{90}_{2\times \sqrt{2}d}$; (g) $III^{90}_{2\times d} \rightarrow III^{90}_{2d,d}$; (h) $III^{90}_{2\times d} \rightarrow III^{90}_{2\times d} \rightarrow III^{135}_{d,\sqrt{2}d}$. The crystal energies of conversion, trapping and motion of adatom clusters are also shown.

Table 1
Activation energies and conversion energies of adatom clusters and atomic vibrational frequencies at 0, 300 and 500 °C

Original position configuration	Final position configuration	Figure	Frequency factor (s^{-1})	Activation energy (eV)	Number of jumps at 0 °C (s^{-1})	Number of jumps at 300 °C (s^{-1})	Number of jumps at 500 °C (s^{-1})
(0, 0, 0) I	(1, 1, 0) I	Fig. 1a	1.23×10^{12}	0.41	3.33×10^{4}	3.05×10^{8}	2.62×10^{9}
(−1, 1, 0)–(0, 0, 0) II_{d}	(−1, 1, 0)–(1, 1, 0) II_{2d}	Fig. 1b	1.03×10^{12}	0.42	1.82×10^{4}	2.09×10^{8}	1.88×10^{9}
(−1, 1, 0)–(1, 1, 0) $II_{d\sqrt{2}}$	(−1, 1, 0)–(0, 0, 0,) II_{d}	Fig. 1b	1.0×10^{12}	0.12	6.71×10^{9}	9.69×10^{10}	1.82×10^{11}
(−1, 1, 0)–(0, 0, 0) II_{d}	(−1, 1, 0)–(1, −1, 0) II_{2d}	Fig. 1c	1.1×10^{12}	0.72	6.12×10^{-2}	6.93×10^{5}	3.19×10^{7}
(−1, 1, 0)–(1, −1, 0) II_{2d}	(−1, 1, 0)–(0, 0, 0) II_{d}	Fig. 1c	1.1×10^{12}	0.27	1.14×10^{7}	4.65×10^{9}	1.91×10^{10}
(−2, 2, 0)–(−1, 1, 0)–(0, 0, 0) $III^{180}_{2\times d}$	(−2, 2, 0)–(−1, 1, 0)–(1, 1, 0) $III^{135}_{d,d\sqrt{2}}$	Fig. 1d	1.1×10^{12}	0.43	1.28×10^{4}	1.82×10^{8}	1.72×10^{9}
(−2, 2, 0)–(−1, 1, 0)–(1, 1, 0) $III^{135}_{d,d\sqrt{2}}$	(−2, 2, 0)–(−1, 1, 0)–(0, 0, 0) $III^{180}_{2\times d}$	Fig. 1d	1.1×10^{12}	0.16	1.17×10^{9}	4.32×10^{10}	1.00×10^{11}
(−2, 2, 0)–(−1, 1, 0)–(1, 1, 0) $III^{135}_{d,d\sqrt{2}}$	(−2, 2, 0)–(−1, 1, 0)–(2, 2, 0) $III^{180}_{d,d\sqrt{2}}$	Fig. 1d	1.35×10^{12}	0.50	6.86×10^{2}	5.49×10^{7}	7.50×10^{8}
(−2, 2, 0)–(−1, 1, 0)–(1, 1, 0) $III^{180}_{d,d\sqrt{2}}$	(−2, 2, 0)–(−1, 1, 0)–(0, 0, 0) $III^{135}_{d,d\sqrt{2}}$	Fig. 1d	1.35×10^{12}	0.16	1.12×10^{11}	5.29×10^{8}	4.26×10^{9}
(−2, 2, 0)–(−1, 1, 0)–(0, 0, 0) $III^{180}_{2\times d}$	(−2, 2, 0)–(−1, 1, 0)–(1, −1, 0) $III^{180}_{d,2d}$	Fig. 1e	1.74×10^{12}	0.69	2.58×10^{-1}	1.52×10^{6}	5.60×10^{7}
(−2, 2, 0)–(−1, 1, 0)–(1, −1, 0) $III^{180}_{d,2d}$	(−2, 2, 0)–(−1, 1, 0)–(0, 0, 0) $III^{180}_{2\times d}$	Fig. 1e	1.35×10^{12}	0.27	1.29×10^{7}	5.74×10^{9}	2.36×10^{10}
(−2, 2, 0)–(−1, 1, 0)–(1, −1, 0) $III^{180}_{d,2d}$	(−2, 2, 0)–(−1, 1, 0)–(2, −2, 0) $III^{180}_{d,3d}$	Fig. 1e	1.35×10^{12}	0.37	1.78×10^{5}	7.60×10^{8}	5.27×10^{9}

diffusion of a single adatom on (1 1 1) surface was quite low [1,2] compared with those for the conversion energies of adatom clusters on (1 1 1), but the values of the activation energies for diffusion on (0 0 1) surface were not very low but those were comparable to the values of the energies of conversion. In this sense, the motion, conversion and break up of adatom clusters mixed together with the motion of single adatoms on (0 0 1). The epitaxial growth on (0 0 1) is more complicated compared with that on (1 1 1). Lee et al. [10] calculated the migration energy of an adatom by ab initio calculation and the results agree with our calculations qualitatively. Papanicolaou et al. [11] obtained 0.43 eV which is very close to our results. Our results are in good agreement with experimental data 0.48 eV [12], 0.28 eV [13], 0.36 eV [14] and 0.30–0.32 eV [15]. We have calculated larger clusters but these will be published in the future. For (1 1 1), we have calculated with the effect of steps and climb up and step down motion were also calculated [1], but in this paper these calculations have not made yet. Reconstruction of the (0 0 1) surface was not taken into account. This problem has to be studied also in the future.

The jump frequency of an adatom can be written as

$$F = f_0 \exp\{-E/[kT]\}$$

We know the vibrational frequency of atoms, f_0, then we can calculate the frequency for the atom to make a jump to a next lattice position. Some of the jump frequencies are listed in Table 1 for 0 and 500 °C.

7. Conclusions

The activation energies of motion and conversion of a gold adatom have been calculated using molecular dynamics and an embedded atom potential at any temperatures. The activation energy for the motion of a gold adatom on (0 0 1) surface of gold is calculated to be 0.41 eV, which is much larger than that for the motion of an adatom on (1 1 1). The activation energies of dissociation in the direction of a di-adatom is 0.72 eV from the nearest neighbor to the next nearest neighbor, and 0.27 eV from the next nearest neighbor to the third nearest neighbor. Butterfly motion of a di-adatom is 0.42 + 0.12 eV = 0.54 eV. Tri-adatoms are classified by the angle between the two bonds in the adatoms and the lengths of the two bonds. The conversion energies of tri-adatoms have also been calculated. These results are shown in Fig. 1 and Table 1. Surface re-constructions were not taken into account in this paper. This problem is left for future work.

References

[1] J. Takano, O. Takai, Y. Kogure, M. Doyama, Thin Solid Films 318 (1998) 52.
[2] M. Doyama, Bull. Mater. Sci. 22 (1999) 835.
[3] M. de Jong, J.S. Koehler, Phys. Rev. 129 (1963) 40.
[4] S.M. Foiles, M.I. Baskes, M.S. Daw, Phys. Rev. B 33 (1986) 7983.
[5] D.J. Oh, R.A. Johnson, J. Mater. Sci. 3 (1988) 471.
[6] D.J. Oh, R.A. Johnson, in: V. Vitek, D.J. Srolovitz (Eds.), Atomic Simulation of Materials, Plenum Press, New York, 1989, p. 233.
[7] G.J. Ackland, G. Tichy, V. Vitek, M.W. Finnis, Phil. Mag. A 56 (1987) 735.
[8] M.I. Baskes, Phys. Rev. B 46 (1992) 2727.
[9] M. Doyama, Y. Kogure, Comput. Mater. Sci. 14 (1999) 80.
[10] C. Lee, G.T. Barkema, M. Breeman, A. Pasquarello, R. Car, Surf. Sci. Lett. 306 (1994) 575.
[11] N.I. Papanicolaou, G.C. Kallinteris, G.A. Evangelakis, in: A. Gonis, et al. (Eds.), Stability of Materials, Plenum Press, New York, 1996, p. 217.
[12] J.J. de Miguel, A. Sanchez, A. Cebollada, J.M. Gallego, J. Ferron, S. Ferrer, Surf. Sci. 189/190 (1987) 1062.
[13] H.J. Ernst, F. Fabre, J. Lapujoulade, Phys. Rev. B 46 (1929) 1992.
[14] M. Breeman, D.O. Boerma, Surf. Sci. 269/27 (1992) 224.
[15] C.L. Lie, J.M. Cohen, J.B. Adams, A.F. Voter, Surf. Sci. 253 (1991) 334.